Double-leaf microperforated panel space absorbers: A revised theory and detailed analysis

Sakagami, Kimihiro
Nakamori, Tomohito
Morimoto, Masayuki
Yairi, Motoki

(Citation)
Applied Acoustics,70(5):703-709

(Issue Date)
2009-05

(Resource Type)
journal article

(Version)
Accepted Manuscript

(URL)
https://hdl.handle.net/20.500.14094/90000848

DOUBLE-LEAF MICROPERFORATED PANEL SPACE ABSORBERS: A REVISED THEORY AND DETAILED ANALYSIS

Kimihiro Sakagami*, Tomohito Nakamori, Masayuki Morimoto
Environmental Acoustics Laboratory, Graduate School of Engineering, Kobe University, Rokko, Nada, Kobe, 657-8501 Japan

and

Motoki Yairi
Kajima Technical Research Institute, Kajima Corp., Chofu, 182-0036 Japan

PACS: 43.55. Ev, 43.55. Dt, 43.50. Gf
Keywords: Microperforated panel (MPP), space absorber, sound absorption

*Corresponding author
Email: saka@kobe-u.ac.jp
Tel/Fax +81 78 803 6043

ABSTRACT

A double-leaf microperforated panel space absorber (DLMPP) is composed of two microperforated panels (MPPs) placed in parallel with an air-cavity in-between, without a back wall or any backing structure. This was proposed as a space sound absorber, which can be used for a sound absorbing screen or partition. A conventional MPP absorber with a rigid back wall is effective only around its resonance frequency, which is usually at middle frequencies, and not effective at low frequencies. However, a DLMPP can be effective also at low frequencies, because an additional sound absorption is produced by its acoustic flow resistance. In the authors' previous work, theoretical analyses on the acoustic properties of a DLMPP were carried out using a simplified electro-acoustical equivalent circuit model. However, the equivalent circuit model includes an approximation, and more sophisticated theory is required for a better prediction and detailed discussion. In this paper, a revised theory for a DLMPP is presented: A Helmholtz integral formulation is employed to obtain a rigorous solution for more precise prediction of the absorptivity of a DLMPP. The result of the present revised theory is compared with that of the equivalent circuit model, and the difference between them is discussed. A parametric survey is made through numerical examples by the present revised theory to discuss its acoustic properties.

INTRODUCTION

A microperforated panel (MPP) absorber, which is composed of a panel with submillimeter holes backed by an air-cavity, is recently recognised as one of the most promising alternatives for next-generation sound absorbing materials because of its fibre-free nature and attractive features. It was first proposed by Maa [1-3]. Its applications, improvement and theoretical development have since been studied extensively [4-7]. It is typically used for ceilings or room interior surfaces, backed by an air-cavity. MPP absorbers can work most efficiently only when they have a back cavity with a back wall, because the sound absorption of an MPP is caused by a Helmholtz-type resonator formed together with them. Therefore, an MPP absorber is effective only in its resonance frequency range. Although it is wider than other resonance type absorbers, but still it is usually limited to about two octaves.

Multiple-leaf MPP absorbers were first proposed by Maa [1-3]: Maa proposed a double-leaf MPP backed by a rigid-back wall with an air-cavity. Recently, Asdrubali and Pispola studied this type of absorber for its application to noise barriers [8]. This absorber is intended to produce two resonators so that a broader absorption frequency range can be obtained. However, as long as an MPP has a back wall, its absorption is caused only by the Helmholtz resonance, and this results in the absorption frequency range limited to its resonance frequency region.

In order to broaden the absorption frequency range, especially to extend it to lower frequencies, it is needed to introduce another absorption mechanism that is effective at low frequencies. Acoustic permeability of MPPs can possibly be utilised for this purpose. A permeable material is known to produce sound absorption by its acoustic flow resistance. A typical example is a single- or multiple-leaf permeable membrane [9-11], which shows moderate absorption (absorbing up to 50% of incident energy) at low frequencies. A similar absorption effect can be expected for MPPs, as an MPP can also be regarded as a permeable material with acoustic flow resistance. Therefore, in the authors' previous study [12], to create an efficient sound-absorbing structure with MPPs alone, a double-leaf MPP *without* a back wall (DLMPP) was proposed and studied with a simplified model.

A DLMPP is composed of two MPPs, placed in parallel with an air-cavity in-between, without a rigid back wall. In this structure, the MPP on the back side plays the role of the back wall in the conventional setting to form the Helmholtz resonator. Thus, a DLMPP is supposed to work as a Helmholtz type absorber at mid-high frequencies, as well as, a permeable structure with acoustic resistance to absorb sound energy at low frequencies. A DLMPP works for sound incident on both sides and can be effectively used as a space absorber or a sound-absorbing panel or screen/partition. This feature can be useful in various situations in which a rigid backing is not available for setting MPPs against, and also it can enable MPPs to be applied to different parts of interior in buildings.

In the previous paper [12], an electro-acoustical equivalent circuit model was used for simplified analysis. Although equivalent circuit analyses are useful to gain a physical insight

into the absorption mechanism, it is inevitable to use an approximate expression for air cavity and this leads to exaggeration of resonance behaviour which causes an error in the results. Therefore, the authors revisited the acoustic properties of DLMPPs with strict theory using a Helmholtz integral formalism. In this paper, the theoretical solution derived from a revised theory based on a Helmholtz integral formalism is introduced. The result of the present revised theory is compared with that of the electro-acoustical equivalent circuit, and the difference between them is discussed. The acoustic characteristics of a DLMPP are discussed by the present revised theory: Numerical examples by the present revised theory are shown to demonstrate the effect of the parameters on the acoustic properties of a DLMPP.

THEORETICAL CONSIDERATIONS

Figure 1 shows the model of a DLMPP for theoretical analysis. MPP1 and 2 are of infinite extent, and they are placed in parallel with an air-cavity of depth D in-between. A plane sound wave of unit pressure amplitude is obliquely incident upon MPP1. Both leaves, MPP1 and 2, have submillimetre perforation which is characterised by the following parameters: hole diameter ($d_{1,2}$), perforation ratio ($\sigma_{1,2}$), and panel thickness (=throat length, $t_{1,2}$). In the analysis the sound induced vibrations of MPP1 and 2 are taken into account, and their vibration displacements are denoted as $w_{1,2}(x)$, respectively. In this model the vibrations of the MPPs are one-dimensional and the sound field becomes two-dimensional. A Helmholtz integral formulation is employed to obtained analytical strict solutions. The time factor is $\exp(-i\omega t)$ and suppressed throughout.

The sound pressures on the illuminated side of MPP1, p_1, and the back side of MPP2, p_3, are expressed by the following Helmholtz integral:

$$p_1(x,0) = 2\,p_i(x,0) + \frac{i}{2}\int_{-\infty}^{\infty} \frac{\partial p_1(x_0,0)}{\partial n} H_0^{(1)}\left(k_0\left|x-x_0\right|\right)dx_0 \,, \tag{1a}$$

$$p_3(x,D) = \frac{i}{2}\int_{-\infty}^{\infty} \frac{\partial p_3(x_0,D)}{\partial n} H_0^{(1)}\left(k_0\left|x-x_0\right|\right)dx_0 \tag{1b}$$

where p_i is the pressure of the incident wave, n is the outward normal of the boundaries, and $H_0^{(1)}$ denoting a Hankel function of the first kind of order zero. The boundary conditions for these surfaces are:

$$\frac{\partial p_1(x_0)}{\partial n} = \rho_0\omega^2 w_1(x) + ik_0 A_{m1}\Delta p_1(x_0)\,, \tag{2a}$$

$$\frac{\partial p_3(x_0)}{\partial n} = -\rho_0\omega^2 w_2(x) - ik_0 A_{m2}\Delta p_3(x_0) \tag{2b}$$

where Δp_1 and Δp_3 are the pressure differences between two surfaces of MPP1 and 2, respectively. $A_{m1,2}=\rho_0 c_0/Z_{1,2}$, with ρ_0 the air density and c_0 the sound speed, ω the angular frequency, and k_0 the wavenumber in air ($=\omega/c_0$). Here, the impedances of the MPPs, $Z_{1,2}=r_{1,2}-i\omega m_{1,2}$ are derived from Maa's formulae [1-3].

$$r_{1,2}=\frac{32\eta}{\sigma_{1,2}\rho_0 c_0}\frac{t_{1,2}}{d_{1,2}^2}\left(\sqrt{1+\frac{\kappa_{1,2}^2}{32}}+\frac{\sqrt{2}}{32}\kappa_{1,2}\frac{d_{1,2}}{t_{1,2}}\right) \tag{3a}$$

$$\omega m_{1,2}=\frac{\omega t_{1,2}}{\sigma_{1,2}c_0}\left(1+\frac{1}{\sqrt{1+\frac{\kappa_{1,2}^2}{2}}}+0.85\frac{d_{1,2}}{t_{1,2}}\right) \tag{3b}$$

where

$$\kappa_{1,2}=\frac{d_{1,2}}{2}\sqrt{\frac{\rho_0\omega}{\eta}} \tag{3c}$$

and η is the dynamic viscosity of the air (17.9 μPa s).

From these equations, the surface pressure on the exposed side of MPP1, p_1 is expressed by a Helmholtz integral as follows:

$$p_1(x,0)=2p_i(x,0)-\frac{1}{2}\int_{-\infty}^{\infty}\left(-i\rho_0\omega^2 w_1(x_0)+k_0 A_{m1}\Delta p_1(x_0)\right)H_0^{(1)}\left(k_0|x-x_0|\right)dx_0 \tag{4}$$

and the surface pressure on the back side of MPP2, p_3, is expressed as:

$$p_3(x,D)=\frac{1}{2}\int_{-\infty}^{\infty}\left(-i\rho_0\omega^2 w_2(x_0)+k_0 A_{m2}\Delta p_2(x_0)\right)H_0^{(1)}\left(k_0|x-x_0|\right)dx_0\ . \tag{5}$$

The pressure and the particle velocity in the cavity are written in the following forms:

$$p_2(x,z)=\left(Xe^{ik_0 z\cos\theta}+Ye^{-ik_0 z\cos\theta}\right)e^{ik_0 x\sin\theta}\quad , \tag{6}$$

$$v_2(x,z)=\frac{\cos\theta}{\rho_0 c_0}\left(Xe^{ik_0 z\cos\theta}-Ye^{-ik_0 z\cos\theta}\right)e^{ik_0 x\sin\theta}\ . \tag{7}$$

The boundary conditions in the cavity, at x=0 and d, respectively, are:

$$v_2(x,0) = -i\omega w_1(x) + \frac{\Delta p_1(x)}{Z_1} \;;\; v_2(x,D) = -i\omega w_2(x) + \frac{\Delta p_3(x)}{Z_2}, \tag{8}$$

Equations (6)-(7) are solved for X and Y, with using (8). X and Y are the pressure amplitudes associated with the waves propagating in the +z and -z directions in the cavity, respectively. Then, the surface pressure on the back side of MPP1 and the cavity side of MPP2 are given as follows:

$$p_2(x,0) = \frac{i\rho_0 c_0 \omega\{(e^{i\varphi} + e^{-i\varphi})w_1(x) - 2w_2(x)\} - \rho_0 c_0\{\frac{\Delta P_1(x)}{Z_1}(e^{i\varphi} + e^{-i\varphi}) - 2\frac{\Delta P_2(x)}{Z_2}\}}{\cos\theta(e^{i\varphi} - e^{-i\varphi})} \tag{9}$$

$$p_2(x,D) = \frac{i\rho_0 c_0 \omega\{2w_1(x) - (e^{i\varphi} + e^{-i\varphi})w_2(x)\} - \rho_0 c_0\{2\frac{\Delta P_1(x)}{Z_1} - (e^{i\varphi} + e^{-i\varphi})\frac{\Delta P_2(x)}{Z_2}\}}{\cos\theta(e^{i\varphi} - e^{-i\varphi})} \tag{10}$$

where $\varphi = k_0 D\cos\theta$.

Now, the displacements $w_{1,2}(x)$ of the sound induced vibrations of MPP leaves are expressed by the following relations using the unit responses of the panel vibration, $u_1(x)$ and $u_2(x)$, for MPP1 and MPP2, respectively:

$$w_1(x) = \int_{-\infty}^{\infty}[p_1(\xi,0) - p_2(\xi,0)]u_1(x-\xi)d\xi, \tag{11}$$

$$w_2(x) = \int_{-\infty}^{\infty}[p_2(\xi,D) - p_3(\xi,D)]u_2(x-\xi)d\xi. \tag{12}$$

Using the Fourier transform technique these equations are transformed, with wavenumber parameter k, into the followings:

$$W_1(k) = 2\pi[P_1(k;0) - P_2(k;0)]U_1(k) \tag{13}$$

$$W_2(k) = 2\pi[P_2(k;D) - P_3(k;D)]U_2(k) \tag{14}$$

where $W_{1,2}(k)$, $P_1(k;0)$ and $P_2(k;d)$ are the transforms of $w_{1,2}(x)$, $p_1(x,0)$ and $p_2(x,d)$, respectively. $U_{1,2}(k)$ are the transform of the unit responses of the vibration of the MPP1 and 2, $u_{1,2}(x)$, which take the following form:

$$U_{1,2}(k) = \frac{1}{2\pi(D_{1,2}k^4 - \rho_{p1,2}t_{1,2}\omega^2)} \tag{15}$$

where $D_{1,2}$ is the flexural rigidity of the MPP leaves, i.e., $D_{1,2}=E_{1,2}t_{1,2}^3(1-i\eta_{1,2})/[12(1-\nu^2_{1,2})]$, with $E_{1,2}$ the Young's modulus, $\rho_{p1,2}$ the plate density, $\eta_{1,2}$ the loss factor and $\nu_{1,2}$ the Poisson's ratio of MPP1 and 2, respectively.

Taking the Fourier transforms of the boundary pressures (4), (5), (9) and (10), and solving them in the wavenumber space, the solutions for the pressures in the wavenumber space are given as follows:

$$P_1(k;0) = 2\delta(k - k_0\sin\theta) + \frac{i\rho_0\omega^2 W_1(k) - k_0 A_{m1}\Delta P_1(k)}{\sqrt{k_0{}^2 - k^2}} \tag{16}$$

$$P_2(k;0) = \frac{\rho_0 c_0\{(e^{i\varphi} + e^{-i\varphi})(i\omega W_1(k) - \frac{\Delta P_1(k)}{Z_1}) - 2(i\omega W_2(k) - \frac{\Delta P_2(k)}{Z_2})\}}{(e^{i\varphi} - e^{-i\varphi})\cos\theta} \tag{17}$$

$$P_2(k;D) = \frac{\rho_0 c_0\{2(i\omega W_1(k) - \frac{\Delta P_1(k)}{Z_1}) - (e^{i\varphi} + e^{-i\varphi})(i\omega W_2(k) - \frac{\Delta P_2(k)}{Z_2})\}}{(e^{i\varphi} - e^{-i\varphi})\cos\theta} \tag{18}$$

$$P_3(k;D) = \frac{-i\rho_0\omega^2 W_2(k) + k_0 A_{m2}\Delta P_2(k)}{\sqrt{k_0{}^2 - k^2}} \tag{19}$$

where δ denotes Dirac's delta function.

Putting these equations into (13) and (14), and solve them for $W_{1,2}(k)$ gives following expressions:

$$W_1(k) = \Gamma_1(k)\delta(k - k_0\sin\theta) \tag{20}$$

$$W_2(k) = \Gamma_2(k)\delta(k - k_0\sin\theta) \tag{21}$$

where

$$\Gamma_1(k) = \frac{-\Phi_1 A_3 + \Phi_1\Phi_2 A_3 B_2 - \Phi_1\Phi_2 A_2 B_3}{-1 + \Phi_1 A_1 + \Phi_1\Phi_2 A_2 B_1 + \Phi_2 B_2 - \Phi_1\Phi_2 A_1 B_2}$$

$$\Gamma_2(k) = \frac{-\Phi_1\Phi_2 A_3 B_1 - \Phi_2 B_3 + \Phi_1\Phi_2 A_1 B_3}{-1 + \Phi_1 A_1 + \Phi_1\Phi_2 A_2 B_1 + \Phi_2 B_2 - \Phi_1\Phi_2 A_1 B_2}$$

with

$$\Phi_1 = 2\pi U_1(k)F_1\,,\ \Phi_2 = 2\pi U_2(k)F_2$$

$$\Theta_1 = \frac{1}{-C_1(F_1F_2 + 4E_1E_2)}, \Theta_2 = \frac{1}{-C_1(G_1G_2 - 4E_1E_2)}$$

$$A_1 = -C_2F_2G + C_1F_2H - 4E_2G\,,\ A_2 = 2C_2E_2G + 2F_2G - 2C_1E_2H\,,\ A_3 = 2C_1F_2$$

$$B_1 = -2F_1G - 2C_2E_1G + 2C_1E_1H\,,\ B_2 = C_2F_1G - C_1F_1H + 4E_1G\,,\ B_3 = 4C_1E_1$$

$$C_1 = (e^{i\varphi} - e^{-i\varphi})\cos\theta\,,\ C_2 = e^{i\varphi} + e^{-i\varphi}$$

$$E_1 = \frac{\rho_0 c_0}{C_1 R_1}\,,\ E_2 = \frac{\rho_0 c_0}{C_1 R_2}$$

$$F_1 = 1 + I_1 - C_2E_1\,,\ F_2 = 1 + I_2 - C_2E_2$$

$$G = i\rho_0 c_0 \omega$$

$$H = \frac{i\rho_0\omega^2}{\sqrt{k_0{}^2 - k^2}}, I_1 = \frac{k_0 A_{m1}}{\sqrt{k_0{}^2 - k^2}}, I_2 = \frac{k_0 A_{m2}}{\sqrt{k_0{}^2 - k^2}}$$

Taking the inverse Fourier transform of $W_{1,2}(k)$, the displacements of the sound induced vibrations of MPP leaves are now given as:

$$w_1(x) = \Gamma_1(k_0 \sin\theta)e^{ik_0 x \sin\theta}\,, \tag{22}$$

$$w_2(x) = \Gamma_2(k_0 \sin\theta)e^{ik_0 x \sin\theta}\,. \tag{23}$$

Once all the boundary values are solved, the reflected pressure p_r and transmitted pressure p_t are obtained (assuming the incident pressure amplitude as unity) as:

$$p_r(x,z) = \left[1 + \frac{i\rho_0\omega^2\Gamma_1(k_0\sin\theta) - k_0 A_{m1}\Theta_1\{A_1\Gamma_1(k_0\sin\theta) + A_2\Gamma_2(k_0\sin\theta) + A_3\}}{k_0\cos\theta}\right] \times \exp[\,i(k_0 x\sin\theta - k_0 z\cos\theta)] \tag{24}$$

$$p_t(x,z) = \frac{-i\rho_0\omega^2\Gamma_2(k_0\sin\theta) + k_0 A_{m2}\Theta_2\{B_1\Gamma_1(k_0\sin\theta) + B_2\Gamma_2(k_0\sin\theta) + B_3\}}{k_0\cos\theta} \times \exp[\,i(k_0 x\sin\theta + k_0 z\cos\theta)] \tag{25}$$

The absorption and transmission coefficients are given as α =1-$|p_r|^2$ and τ =$|p_t|^2$, respectively. As a DLMPP is a space absorber and it causes sound transmission, it is necessary to eliminate the effect of transmission from the absorption coefficient for evaluating its absorption efficiency. Therefore, the difference of these coefficients, $\alpha-\tau$, which indicates the ratio of the energy dissipated in the system, is used to evaluate the absorptivity unless otherwise noted.

NUMERICAL EXAMPLES AND DISCUSSION

Comparison with electro-acoustical equivalent circuit model

Figure 2 shows an example of the absorptivity ($\alpha-\tau$) of a DLMPP calculated by the present theory (Eqs. (24) and (25)), in comparison with that calculated by the electro-acoustical equivalent circuit model. As described above, the equivalent circuit model can tend to exaggerate the resonance behaviour of the air cavity, so that the result tend to show a larger absorption peak. Also, the resonance peak appears at somewhat lower frequencies than the present theory. This implies that the equivalent circuit analysis can overestimate the resonance absorption, but as shown in the figure, there is no difference at low frequencies: The low frequency absorption is caused by the acoustic resistance of the MPP leaves and the air cavity does not contribute to it.

These differences between two calculation methods will cause a difference in the prediction of optimal parameter ranges: Figures 3 and 4 show the relationships (contour line) of the acoustic resistance (normalised to $\rho_0 c_0$) of an MPP leaf and the field-incidence-averaged absorptivity ($\alpha-\tau$) at each frequency calculated by the present revised theory and the electro-acoustical equivalent circuit model, respectively. The calculations were made, assuming the two leaves to have the same parameters, with setting the reactance of the MPP ωm=0 and with its resistance, r, being a parameter. Therefore, these figures show the relationships between the resistance of the MPP, r, and the absorptivity at each frequency. Note that these figures do not show how the absorptivity behave to a particular hole parameter such as hole diameter, perforation ratio etc, but they show the global behaviour of absorptivity to the resistance. Bright zone shows high absorptivity.

At low frequencies, the resistance giving the maximum absorptivity depends on frequency: The value decreases with decreasing frequency, and also with decreasing surface density of an MPP due to the effect of the sound induced vibration. On the contrary, at high frequencies, especially at the resonance peak frequency range, the value do not change very much with the surface density.

At the peak frequency range, as shown in Fig. 3, bright zone (=high absorptivity) appears when the resistance is around $2.25\rho_0 c_0$, but in Fig. 4 it appears when it is around $1.5\rho_0 c_0$. This means that the maximum absorption appears when the resistance is 1.5 $\rho_0 c_0$ in electro-acoustical equivalent circuit model, but $2.25\rho_0 c_0$ in the present theory, which means these theories give different prediction for optimal parameters: the optimal acoustic resistance maximising the absorptivity will be higher with the present theory than that with the equivalent circuit model. This may be of some importance in designing process, though the absorptivity is not very sensitive to small change in the resistance.

Parametric survey

Figure 5 shows the effect of the hole diameter (d) of MPPs on the absorption characteristics ($\alpha-\tau$) of a DLMPP. In this example, the absorption peak at the Helmholtz resonance is maximised at around 1.5 kHz when the diameter is 0.15 mm. Smaller or larger diameters give lower peak values. At low frequencies the absorptivity becomes the highest at d=0.2 mm. The low frequency absorption decreases at around 125 Hz in all cases. This decrease is because the acoustic resistance of the leaves is decreased by the effect of their sound induced vibration. The optimal value of hole diameter therefore is around 0.15...0.2 mm.

Of course, the optimal value of each parameter changes accordingly by the effect of the vibration. But, these tendencies in principle depend on the behaviour of the acoustic resistance of MPP leaves, $r_{1,2}$, and the optimal value of each parameter depends on the other parameters. Therefore, similar tendencies are observed when the other parameters, e.g., thickness and perforation ratio, are changed. Regarding the perforation ratio, it also affects the peak frequency: larger perforation ratio gives higher peak frequency, though too large perforation ratio cannot offer effective peak absorption (Fig. 6).

The peak frequency can be mainly controlled by the cavity depth (Fig. 7). The resonance peak is shifted to higher frequencies as the cavity depth decreases. The peak value decreases as the peak frequency shifts to higher frequencies. A similar tendency is observed in the case of a double-leaf MPP with a rigid back wall. This is attributed to the acoustic reactance of the MPP, $\omega m_{1,2}$, which increases with frequency: it affects the total acoustic reactance of the system. This result suggests that there is a frequency range in which a DLMPP shows the most effective absorptivity.

Since the low frequency absorption depends on the total acoustic resistance, not only those MPP parameters but the mass of the MPP leaves is also important. As known in other permeable structures such as a permeable membrane, the acoustic resistance decreases with decreasing its surface density owing to the sound induced vibration. Figure 8 shows the effect of the surface density of MPPs on the absorption characteristics of a DLMPP. Lightweight MPPs give very small absorption at low frequencies. When the surface density is larger than 2.0 kg/m^2, the characteristics are almost the same as those for immobile leaves. Therefore, to make a DLMPP effective at low frequencies, it is necessary to use an MPP of appropriate weight.

CONCLUDING REMARKS

In this paper, the acoustic properties of a double-leaf microperforated panel space absorber (DLMPP) without backing structure was revisited with a revised theory. The revised theory is formalised by a Helmholtz integral and gives strict solutions to the acoustic properties of a DLMPP. In the revised theory the resonant behaviour in the cavity is not so exaggerated as is observed in conventional electro-acoustical equivalent circuit model. Therefore, the revised

theory gives lower resonant peak than equivalent circuit model. According to the present revised theory the resistance of an MPP giving the maximum absorption at the resonance peak is $2.25\rho_0 c_0$, whereas it becomes $1.5\ \rho_0 c_0$ according to the electro-acoustical equivalent circuit model analysis. Parametric survey has been performed to present the effect of each parameter in DLMPP. Experimental validation and further experimental results, including a discussion on further improvement of DLMPPs will be presented in the sequel.

ACKNOWLEDGEMENTS

The authors wish to thank Dr Atsuo Minemura for his valuable discussion. They also thank Dr Nicole Kessissoglou at the University of New South Wales for her constructive comments on this work.

References

[1] Maa D-Y. Theory and design of microperforated panel sound-absorbing constructions. Scientia Sinica 1975; 17: 55-71.

[2] Maa D-Y. Microperforated-panel wideband absorber. Noise Control Eng. J. 1987; 29: 77-84.

[3] Maa D-Y. Potential of microperforated panel absorber. J. Acoust. Soc. Am. 1998; 104: 2861-2866.

[4] Fuchs HV, Zha X. Einsatz mikro-perforierter Platten als Schallabsorber mit inharenter Dampfung. Acustica 1995; 81: 107-116.

[5] Zha X, Fuchs HV, Drotleff HD. Improving the acoustic working conditions for musicians in small spaces. Applied Acoustics 2002; 63: 203-221.

[6] Wu MQ. Micro-perforated panels for duct silencing. Noise Control Eng. J. 1997; 45: 69-77.

[7] Kang J, Brocklesby MW. Feasibility of applying micro-perforated absorbers in acoustic window systems. Applied Acoustics 2005; 66: 669-689.

[8] Asdrubali F, Pispola G. Properties of transparent sound-absorbing panels for use in noise barriers. J. Acoust. Soc. Am. 2007; 121: 214-221.

[9] Takahashi D, Sakagami K, Morimoto M. Acoustic properties of permeable membranes. J. Acoust. Soc. Am. 1996; 99: 3003-3009.

[10] Sakagami K, Kiyama M, Morimoto M, Takahashi D. Detailed analysis of acoustic properties of a permeable membrane. Applied Acoustics 1998; 54: 93-111.

[11] Sakagami K, Morimoto M, Kiyama M. Membrane and membrane structures for acoustical applications: an overview. CD-ROM proceedings of WESPAC VIII, Melbourne, Australia, 2003.

[12] Sakagami K, Morimoto M, Koike W. A numerical study of double-leaf microperforated panel absorbers. Applied Acoustics 2006; 67: 609-619.

[13] Yairi M, Sakagami K, Morimoto M. Double-leaf microperforated panel space absorbers: An experimental study for further improvement. CD-ROM Proceedings of the 19th International Congress on Acoustics, Madrid, Spain, 2007.

Captions of figures

Figure 1. Model of a DLMPP for theoretical analyses. Z_1 and Z_2 are the impedances, and M_1 and M_2 are the surface densities of MPP1 and 2, respectively.

Figure 2. Comparison of the field-incidence averaged absorptivity (a-t) calculated by the present theory and equivalent circuit theory for a DLMPP. Hole diameter: 0.2 mm, Thickness: 0.4 mm, Perforation ratio: 1.0%, Surface density: 1.0 kg/m^2, Cavity depth: 50 mm, for both MPP1 and 2. (1) Present theory, (2) Equivalent circuit theory.

Figure 3. Relationship of acoustic resistance (normalised to air impedance) of an MPP leaf and the absorptivity (α–τ, contour line) at each frequency calculated by the present revised theory. Bright zone shows high absorptivity. (a) immobile case, (b) M=10 kg/m^2, (c) M=3 kg/m^2, and (d) M=1 kg/m^2.

Figure 4. Relationship of acoustic resistance (normalised to air impedance) of an MPP leaf and the absorptivity (α–τ, contour line) at each frequency calculated by the electro-acoustical equivalent circuit model. Bright zone shows high absorptivity. (a) immobile case, (b) M=10 kg/m^2, (c) M=3 kg/m^2, and (d) M=1 kg/m^2.

Figure 5. Effect of hole diameter on the field-incidence-averaged absorptivity (α–τ) of a DLMPP. Hole diameter d=0.1 (1), 0.15 (2), 0.2 (3), and 0.3 (4) mm. Two leaves are given the same parameters. Thickness: 0.4 mm, Perforation ratio: 1.0%, Surface density: 1.0 kg/m^2, Cavity depth: 50mm

Figure 6. Effect of perforation ratio on the field-incidence-averaged absorptivity (α–τ) of a DLMPP. Perforation ratio p= 0.25% (1), 0.5% (2), 1.0% (3), and 2.0%. Two leaves are given the same parameters. Hole diameter: 0.2 mm, Thickness: 0.4 mm, Surface density: 1.0 kg/m^2, Cavity depth: 50mm.

Figure 7. Effect of cavity depth on the field-incidence-averaged absorptivity (α–τ) of a DLMPP. Cavity depth D= 12.5 (1), 25 (2), 50 (3), and 75 (4) mm. Two leaves are given the same parameters. Hole diameter: 0.2 mm, Perforation ratio: 1.0%, Thickness: 0.4 mm, Surface density: 1.0 kg/m^2.

Figure 8. Effect of surface density of MPPs on the field-incidence-averaged absorptivity (α–τ) of a DLMPP. Surface density M= 0.25 (1), 0.5 (2), 1.0 (3) and 2.0 (4) kg/m^2. Two leaves are given the same parameters. Hole diameter: 0.2 mm, Perforation ratio: 1.0%, Thickness: 0.4 mm. Cavity depth: 50 mm.

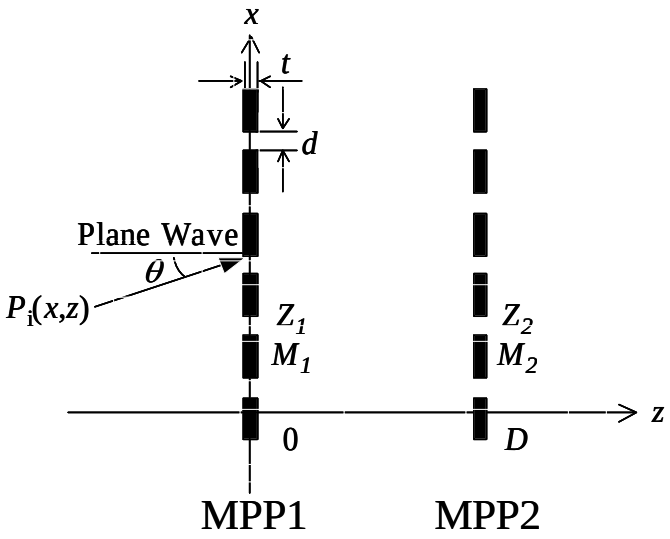

Figure 1. Model of a DLMPP for theoretical analyses. Z_1 and Z_2 are the impedances, and M_1 and M_2 are the surface densities of MPP1 and 2, respectively.

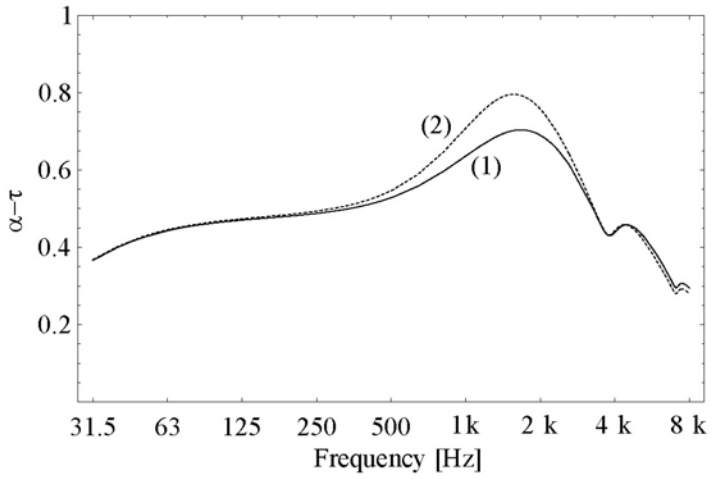

Figure 2. Comparison of the field-incidence averaged absorptivity (*a*-*t*) calculated by the present theory and equivalent circuit theory for a DLMPP. Hole diameter: 0.2 mm, Thickness: 0.4 mm, Perforation ratio: 1.0%, Surface density: 1.0 kg/m^2, Cavity depth: 50 mm, for both MPP1 and 2. (1) Present theory, (2) Equivalent circuit theory.

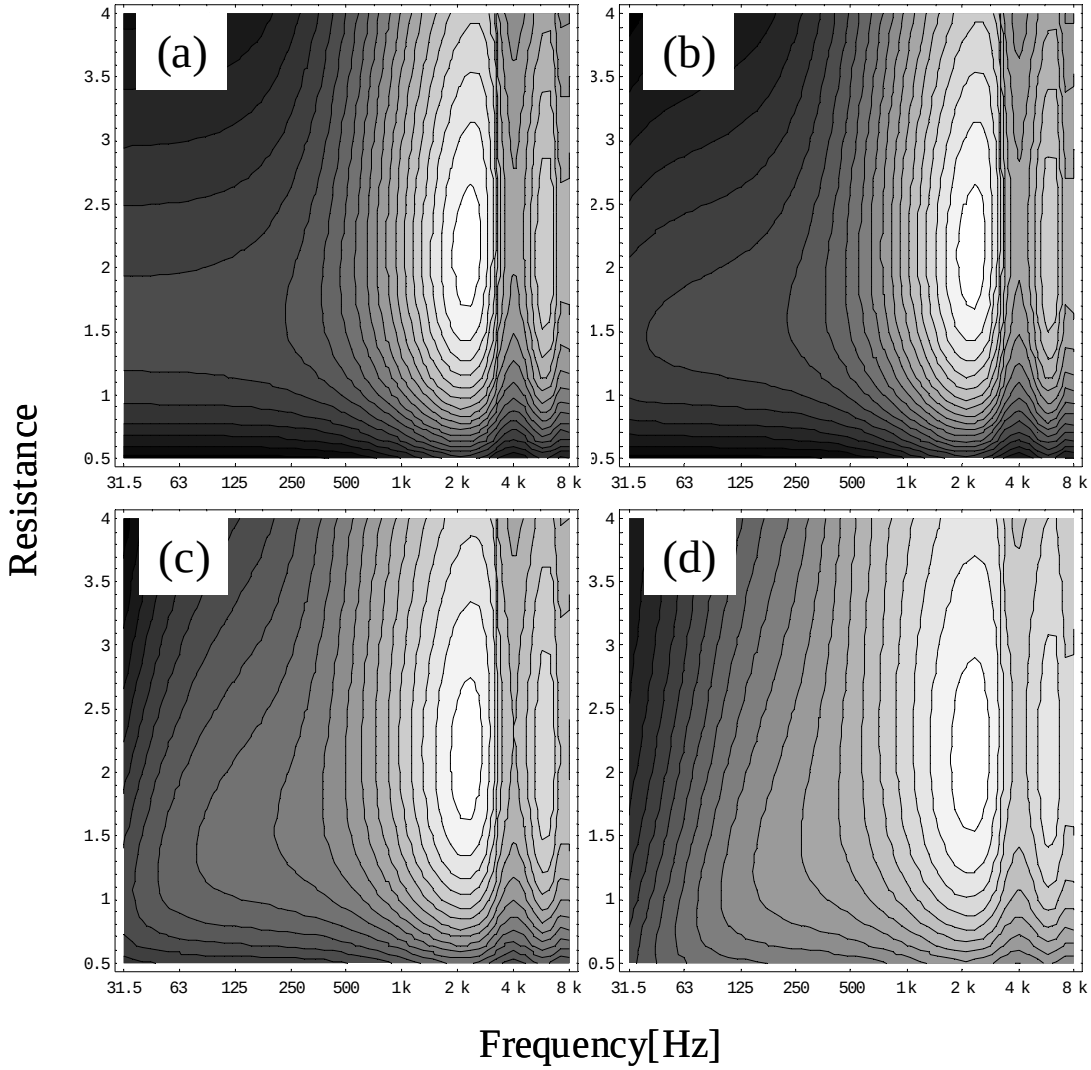

Figure 3. Relationship of acoustic resistance (normalised to air impedance) of an MPP leaf and the absorptivity ($\alpha-\tau$, contour line) at each frequency calculated by the present revised theory. Bright zone shows high absorptivity. (a) immobile case, (b) M=10 kg/m^2, (c) M=3 kg/m^2, and (d) M=1 kg/m^2.

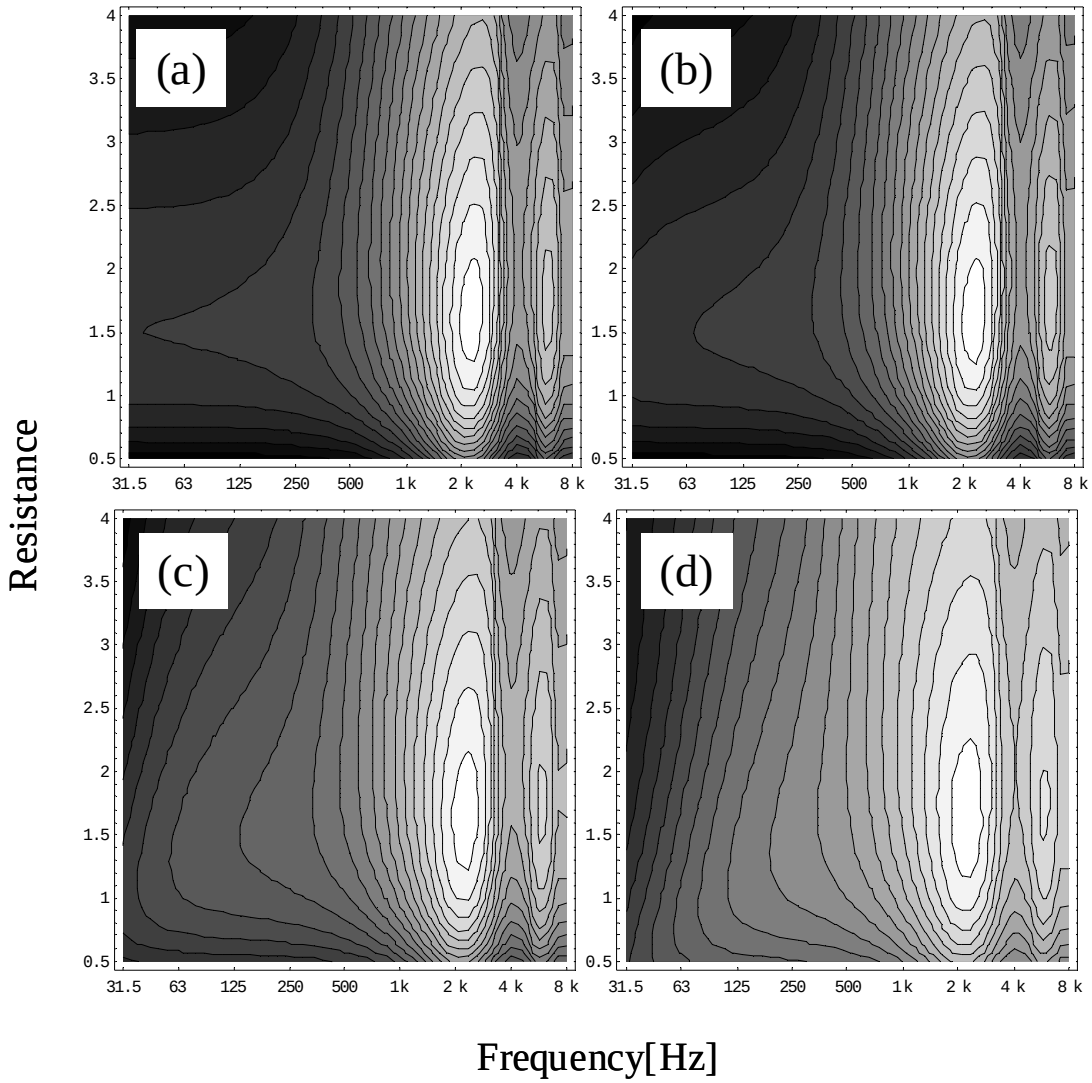

Figure 4. Relationship of acoustic resistance (normalised to air impedance) of an MPP leaf and the absorptivity (α–τ, contour line) at each frequency calculated by the electro-acoustical equivalent circuit model. Bright zone shows high absorptivity. (a) immobile case, (b) M=10 kg/m^2, (c) M=3 kg/m^2, and (d) M=1 kg/m^2.

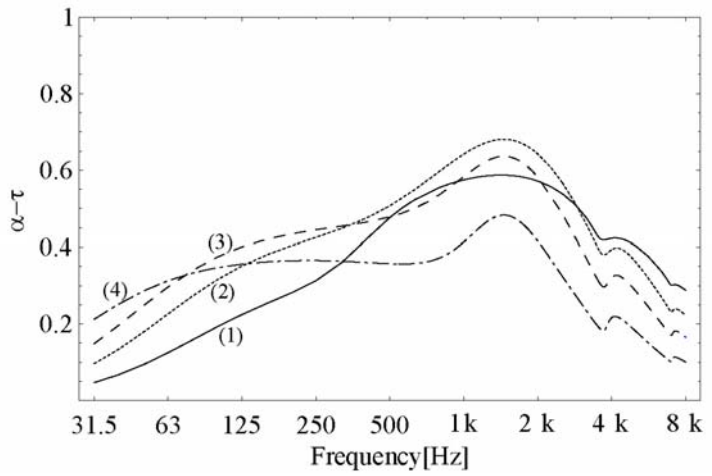

Figure 5 Effect of hole diameter on the field-incidence-averaged absorptivity ($\alpha-\tau$) of a DLMPP. Hole diameter d=0.1 (1), 0.15 (2), 0.2 (3), and 0.3 (4) mm. Two leaves are given the same parameters. Thickness: 0.4 mm, Perforation ratio: 1.0%, Surface density: 1.0 kg/m^2, Cavity depth: 50mm

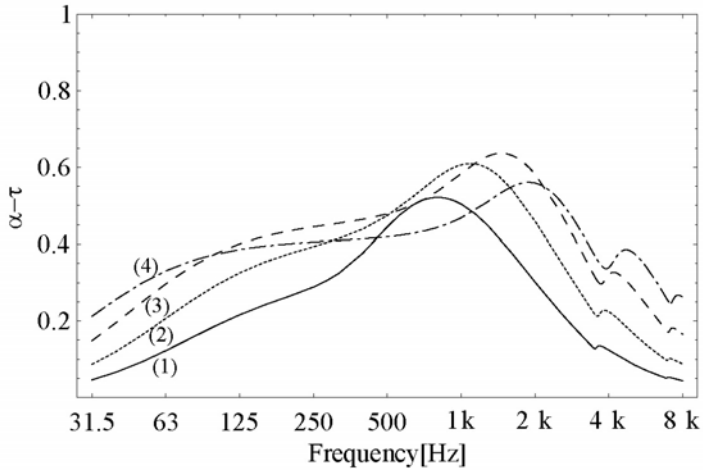

Figure 6. Effect of perforation ratio on the field-incidence-averaged absorptivity ($\alpha-\tau$) of a DLMPP. Perforation ratio p= 0.25% (1), 0.5% (2), 1.0% (3), and 2.0%. Two leaves are given the same parameters. Hole diameter: 0.2 mm, Thickness: 0.4 mm, Surface density: 1.0 kg/m^2, Cavity depth: 50mm.

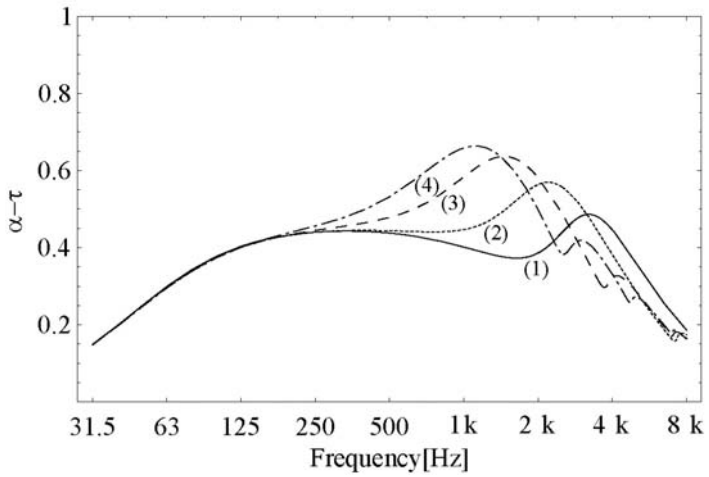

Figure 7. Effect of cavity depth on the field-incidence-averaged absorptivity ($\alpha-\tau$) of a DLMPP. Cavity depth D= 12.5 (1), 25 (2), 50 (3), and 75 (4) mm. Two leaves are given the same parameters. Hole diameter: 0.2 mm, Perforation ratio: 1.0%, Thickness: 0.4 mm, Surface density: 1.0 kg/m^2.

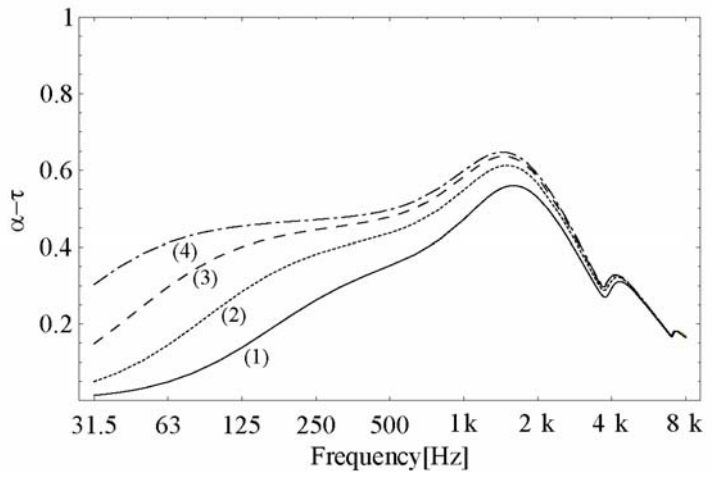

Figure 8. Effect of surface density of MPPs on the field-incidence-averaged absorptivity ($\alpha-\tau$) of a DLMPP. Surface density M= 0.25 (1), 0.5 (2), 1.0 (3) and 2.0 (4) kg/m^2. Two leaves are given the same parameters. Hole diameter: 0.2 mm, Perforation ratio: 1.0%, Thickness: 0.4 mm. Cavity depth: 50 mm.